Dimeric PKD regulates membrane fission to form transport carriers at the TGN

Carine Bossard,[1] Damien Bresson,[2] Roman S. Polishchuk,[3] and Vivek Malhotra[1]

[1]Section of Cell and Developmental Biology, University of California, San Diego, La Jolla, CA 92093
[2]La Jolla Institute for Allergy and Immunology, Developmental Immunology 3, La Jolla, CA 92037
[3]Department of Cell Biology and Oncology, Consorzio Mario Negri Sud, Santa Maria Imbaro (CH) 66030, Italy

Protein kinase D (PKD) is recruited to the trans-Golgi network (TGN) through interaction with diacylglycerol (DAG) and is required for the biogenesis of TGN to cell surface transport carriers. We now provide definitive evidence that PKD has a function in membrane fission. PKD depletion by siRNA inhibits trafficking from the TGN, whereas expression of a constitutively active PKD converts TGN into small vesicles. These findings demonstrate that PKD regulates membrane fission and this activity is used to control the size of transport carriers, and to prevent uncontrolled vesiculation of TGN during protein transport.

Introduction

To understand the mechanism of membrane fission, we identified and used a compound called Ilimaquinone (IQ), which vesiculates the Golgi apparatus via a trimeric G protein subunit βγ and a serine/threonine kinase called protein kinase D (PKD)–dependent process (Takizawa et al., 1993; Jamora et al., 1997, 1999). Importantly, PKD is necessary for the biogenesis of TGN to cell surface transport carriers (Liljedahl et al., 2001; Bard and Malhotra, 2006). The binding of PKD to TGN requires DAG (Baron and Malhotra, 2002) and is activated by Golgi-associated PKCη (Diaz Anel and Malhotra, 2005). PKD activates the lipid kinase activity of PI4kinase IIIß to generate phosphoinositide 4-phosphate (PI4P) from PI, and regulates the binding of ceramide transfer protein CERT to PI4P. PI4P is required for TGN-to-cell surface transport (Walch-Solimena and Novick, 1999; Audhya et al., 2000; Godi et al., 2004; Hausser et al., 2005, 2006; Fugmann et al., 2007). The evidence for PKD's role in the formation of TGN to cell surface transport carriers is though use of a kinase-dead (KD) form and pharmacological inhibitors. The best evidence for PKD's direct involvement in membrane fission requires that its depletion inhibits protein secretion. However, the problem is exacerbated by the fact that there are three isoforms of PKD in the mammalian cells (1, 2, and 3) (Rykx et al., 2003), and all are involved in the formation of basolaterally directed transport carriers (Yeaman et al., 2004). We believe we have now addressed this issue. Our findings reveal that HeLa cells contain predominantly PKD2 and PKD3, and virtually no PKD1. PKD2 and PKD3 dimerize at the TGN and we suggest they activate different substrates. Importantly, depletion of PKD2 and PKD3 by siRNA inhibits TGN-to-cell surface transport. Under these conditions, cargo containing tubules and reticular membranes accumulate at the TGN. In contrast, overexpression of an activated PKD causes extensive vesiculation of TGN. These results demonstrate convincingly that PKD is a bona fide component of membrane fission used to regulate the number and size of TGN-to-cell surface transport carriers depending on the physiological (cargo) needs.

Correspondence to Vivek Malhotra: vivek.malhotra@crg.es

V. Malhotra's present address is Cell and Developmental Biology program, Centre de Regulació Genòmica (CRG), Dr. Aiguader 88, 08003 Barcelona, Spain.

Abbreviations used in this paper: CA, constitutively active; KD, kinase dead; PKD, protein kinase D; PLAP, placental alkaline phosphatase; SS, signal sequence; ST, sialyltransferase.

Results and discussion

Depletion of PKD2 and PKD3 inhibits TGN-to-cell surface protein transport

RT-PCR–based analysis revealed that of the three PKD isoforms, only PKD2 and PKD3 were expressed in HeLa cells (Fig. 1 A). These results were confirmed by quantitative RT-PCR (qRT-PCR): PKD1-specific mRNA is virtually undetectable (10- and 12-fold lower) compared with PKD2 and PKD3, respectively (Fig. 1 B). Specific siRNAs were designed to deplete PKD2 and PKD3 in HeLa cells. Western blotting with specific antibodies revealed a 70–75% reduction in the level of PKD2 and PKD3, respectively (Fig. 1, C and E). By comparison, the level of β-actin was not affected by PKD-specific siRNAs (Fig. 1 D).

To test the effect of PKD2 and PKD3 depletion on protein secretion, control cells and depleted HeLa cells were cotransfected with a plasmid expressing HRP containing the N-terminal signal sequence (SS) as described previously (Bard et al., 2006)

© The Rockefeller University Press $30.00
The Journal of Cell Biology, Vol. 179, No. 6, December 17, 2007 1123–1131
http://www.jcb.org/cgi/doi/10.1083/jcb.200703166

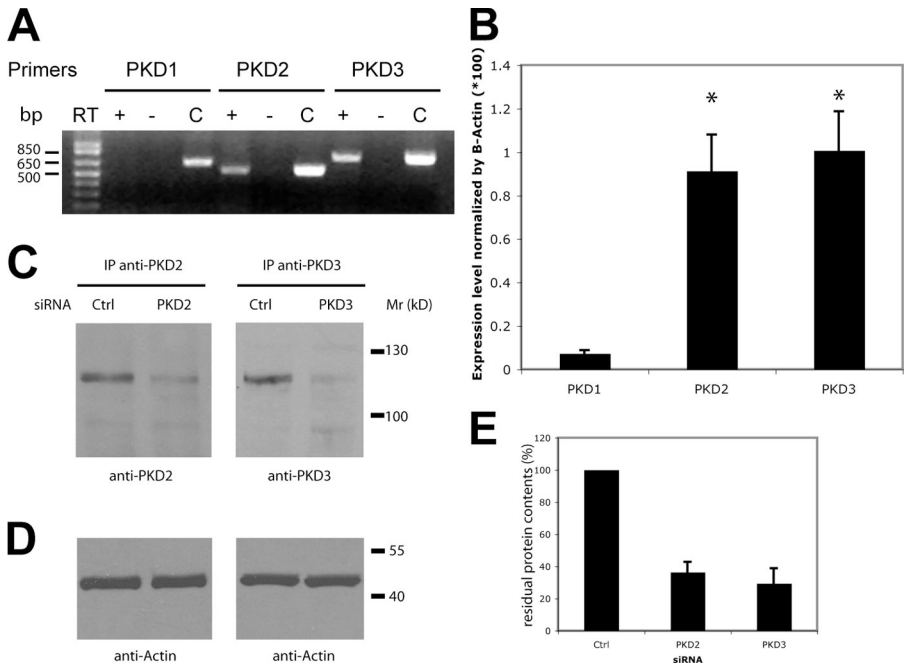

Figure 1. **Relative expression of PKD isoforms in HeLa cells and their depletion by siRNA.** (A) Analysis of mRNA expression by RT-PCR shows that PKD2 and PKD3 are the only PKD isoforms expressed in HeLa cells. RT-PCR reaction without the reverse transcriptase (RT−) was used as a negative control and PCR with the corresponding PKD cDNA (C) as a positive control. (B) Quantitative real-time RT-PCR analysis was performed on RNA extracted from HeLa cells. Bars represent the mean (±SD) of the relative mRNA expression of each PKD isoform compared with the average expression of β-actin. *, $P < 0.01$ compared with PKD1. (C) PKD2 and PKD3 protein levels in HeLa cells transfected with the indicated siRNA were detected by immunoblot analysis after immunoprecipitation from 100 μg of cell lysate using anti-PKD2 and anti-PKD3 antibodies, respectively. (D) β-Actin expression in the lysates used for immunoprecipitation was monitored as a loading control. (E) The effect of PKD2 and PKD3 siRNA was quantified by densitometry and normalized to the expression of PKD2 and PKD3, respectively, in cells transfected with control siRNA.

together with a plasmid expressing placental alkaline phosphatase (PLAP), a GPI-anchored protein that contains an apical sorting signal (Lisanti et al., 1990; Lipardi et al., 2000). The activities of HRP and PLAP released into the medium were measured by chemiluminescence (Bard et al., 2006). HRP secretion is inhibited by 82% in cells transfected by PKD2 siRNA and by 80% in cells transfected by PKD3 siRNA compared with control siRNA-transfected cells (Fig. 2 A). None of the PKD siRNAs have any effect on PLAP secretion (Fig. 2 B). These findings strengthen our previous proposal that similarly to polarized cells that have distinct apical and basolateral targeting pathways, nonpolarized HeLa cells sort proteins into apical-like (PKD-independent) and basolateral-like (PKD-dependent) pathways (Yeaman et al., 2004). Simultaneous depletion of PKD2 and PKD3 from HeLa cells did not have a synergistic effect in inhibiting HRP secretion (unpublished data). Because siRNA-based depletion is not complete, we suggest the residual PKD is sufficient to support trafficking from the TGN to the cell surface. To further ascertain the involvement of PKD2 and PKD3 in trafficking, their involvement in the transport of vesicular stomatitis virus (VSV)–G protein was monitored. HeLa cells were first cotransfected with either siRNA specific for PKD2, PKD3, or a control, and a fluorescent-labeled siRNA to identify transfected cells. After 30 h, the cells were transfected with the tsO45 strain of VSV-G–GFP, which has a thermosensitive mutation causing it to unfold in the ER at the nonpermissive temperature of 39.5°C. Upon shifting cells to the permissive temperature of 32°C, tsO45VSV-G protein folds and is transported to the cell surface. The amount of VSV-G at the cell surface was quantified by immunofluorescence flow cytometry permitting analysis of more than 5,000 cells transfected with both siRNA and VSV-G-GFP. In control cells, VSV-G protein was found at the cell surface within 40 min of shift to 32°C. In PKD2- and PKD3-depleted cells (either individually or together), 50% less VSV-G was found at the cell surface (Fig. 2 C). This is a significant effect on the trafficking of VSV-G to the cell surface considering that siRNA-based depletion of PKD is not complete, and the residual levels (25–30%) would support trafficking, albeit at a slower rate.

Immunoelectron microscopy was used to monitor effects on the secretion of ss-HRP (cargo) in cells depleted of PKD2 and PKD3. Compared with control cells (Fig. 2 D), PKD2 and PKD3 depletion resulted in accumulation of HRP containing highly fenestrated membranes, and large tubules in the trans region of the Golgi stacks (Fig. 2, E and F). To quantitate the number of tubules in the TGN, 20 different Golgi stacks were visualized. In control cells there were 1 to 3 tubules per stack, whereas in PKD-depleted cells the number of tubules increased to 3 to 6 per stack. In sum, PKD depletion results in accumulation of HRP in the TGN and on average a 2.9-fold increase in the number of HRP-containing tubules per Golgi stack. We suggest that these tubules and fenestrated HRP-containing membranes would ordinarily be converted into small transport carriers by membrane fission. However, depletion of PKD2 and PKD3 inhibits events leading to membrane fission, thus accumulating cargo (in this instance HRP) in tubular elements.

PKD2 and PKD3 dimerize in vitro and in vivo and transphosphorylate

Why does depletion of either PKD2 or PKD3 affect Golgi-to-cell surface transport? Why is the other (nondepleted) isoform not functional under such conditions? Do these forms dimerize to activate downstream targets? To test this hypothesis, PKD2 and PKD3 were immunoprecipitated separately from HeLa cell lysates and Western blotted with anti-PKD3 and anti-PKD2, respectively. Western blotting pure recombinant PKD2 and 3 confirmed the specificity of the antibodies to PKD2 and PKD3 (Fig. 3 A). The endogenous PKD2 and PKD3 were found to coprecipitate (Fig. 3 B). Exogenously expressed GST-PKD2 and Flag-PKD3 also coprecipitate specifically (Fig. 3 C). GST alone

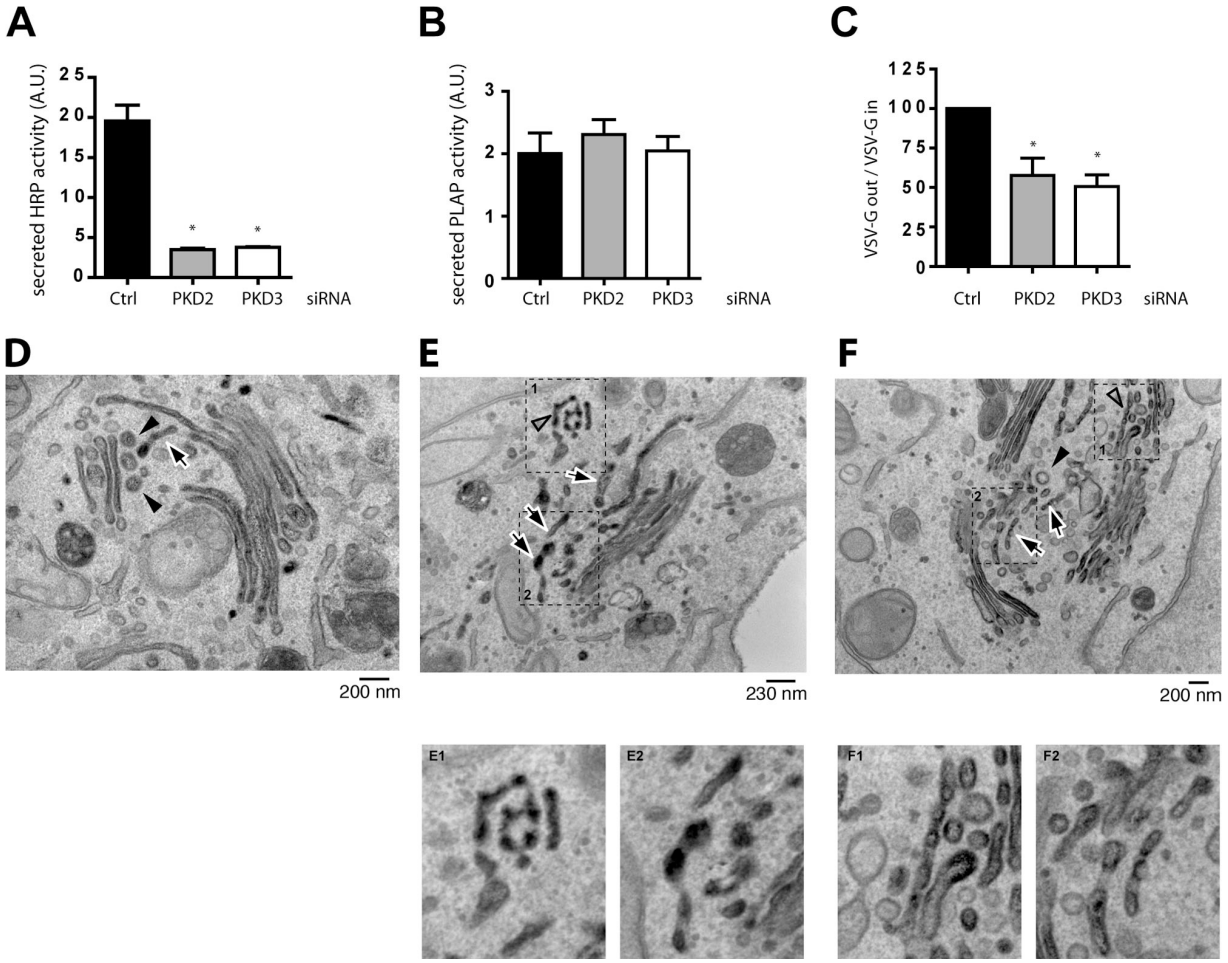

Figure 2. **Depletion of PKD2 or PKD3 inhibits secretion of ss-HRP.** (A and B) ss-HRP and PLAP cDNAs were cotransfected in HeLa cells depleted or not of PKD2 or PKD3. 20 h after transfection, HRP activity secreted in the medium was measured by chemiluminescence. PLAP activity in cell lysates and secreted into the medium was measured as described in Materials and methods. Bars represent the mean ± SD of HRP (A) or PLAP (B) activity in the medium normalized by PLAP activity in cell lysates/total protein concentration. (C) Depletion of PKD2 or PKD3 inhibits VSV-G transport. *tso45*VSV-G-GFP plasmid was transfected in HeLa cells depleted or not of PKD2 or PKD3. The levels of VSV-G at the cells surface and inside the cells were determined by FACS analysis. The bars represent the relative ratio of VSV-G at the surface to the total expressed in depleted cells compared with siRNA control transfected cells ± SEM. *, $P < 0.01$ compared with the control. (D–F) PKD2- and PKD3-depleted HeLa cells and control cells were transfected with ss-HRP and the organization of the Golgi membranes and the localization of HRP monitored by electron microscopy. In control cells (D), the arrow indicates a single tubular profile and arrowheads indicate round profiles (presumably vesicles) in the trans-Golgi region. In contrast, in PKD2- and PKD3-depleted cells (E and F), HRP accumulates in tubular membranes. The arrows indicate multiple tubular profiles at the TGN. The open arrowheads show pearling tubules. The arrowhead in F is a clathrin-coated vesicle revealing the trans side of the Golgi stack.

does not coprecipitate with Flag-PKD3, and Flag-HRP used as a negative control for Flag-tagged protein does not coprecipitate with GST-PKD2. It is interesting to note that Flag-PKD3 construct, when expressed, co-migrates with a fragment of a 34-kD apparent molecular weight. This product is specific for PKD3 because it only appears when Flag-PKD3 is expressed. Because the Flag tag is present at the N-terminal part of PKD3, this 34-kD fragment is a degradation product of PKD3 containing its cysteine-rich domain. More interestingly, this degradation product (Flag-PKD3-Nterm) is also coimmunoprecipitated with GST-PKD2 (Fig. 3 C, top right panel), suggesting that PKD3's cysteine-rich domain binds PKD2. Purified, recombinant-tagged PKD2 and 3 incubated in vitro also coprecipitate, which reveals a direct interaction between PKD2 molecules, PKD3 molecules, and between PKD2 and PKD3 (Fig. 3 D).

PKDs cycle between cytosol and the TGN. A kinase-dead form binds to the TGN but fails to dissociate. Under such conditions, cargo-filled transport carriers form but fail to detach and grow into large tubules. PKD-KD is found both on the TGN and the tubules. Flag-PKD2-KD and GST-PKD3-WT were expressed in HeLa cells and the cells stained with anti-PKD2 and anti-GST antibody. Flag-PKD2-KD was localized to the TGN and the tubules and more interestingly, so was PKD3-WT. Similarly, in cells expressing GST-PKD3-KD, Flag-PKD2-WT was found on the TGN and the tubules (Fig. 3 E). These findings further strengthen our arguments that PKD2 and PKD3 form a dimer and reveal for the first time the localization of the wild-type kinase on the TGN and the TGN-derived tubules, when the corresponding partner is a kinase-inactive form. The fact that these tubules do not detach indicates that both kinases have to be functionally active for membrane fission. The binding of PKD to the Golgi membranes requires DAG (Baron and Malhotra, 2002). However, PKD2 and PKD3 can interact in cells depleted of DAG (unpublished data). These findings reveal that PKD2

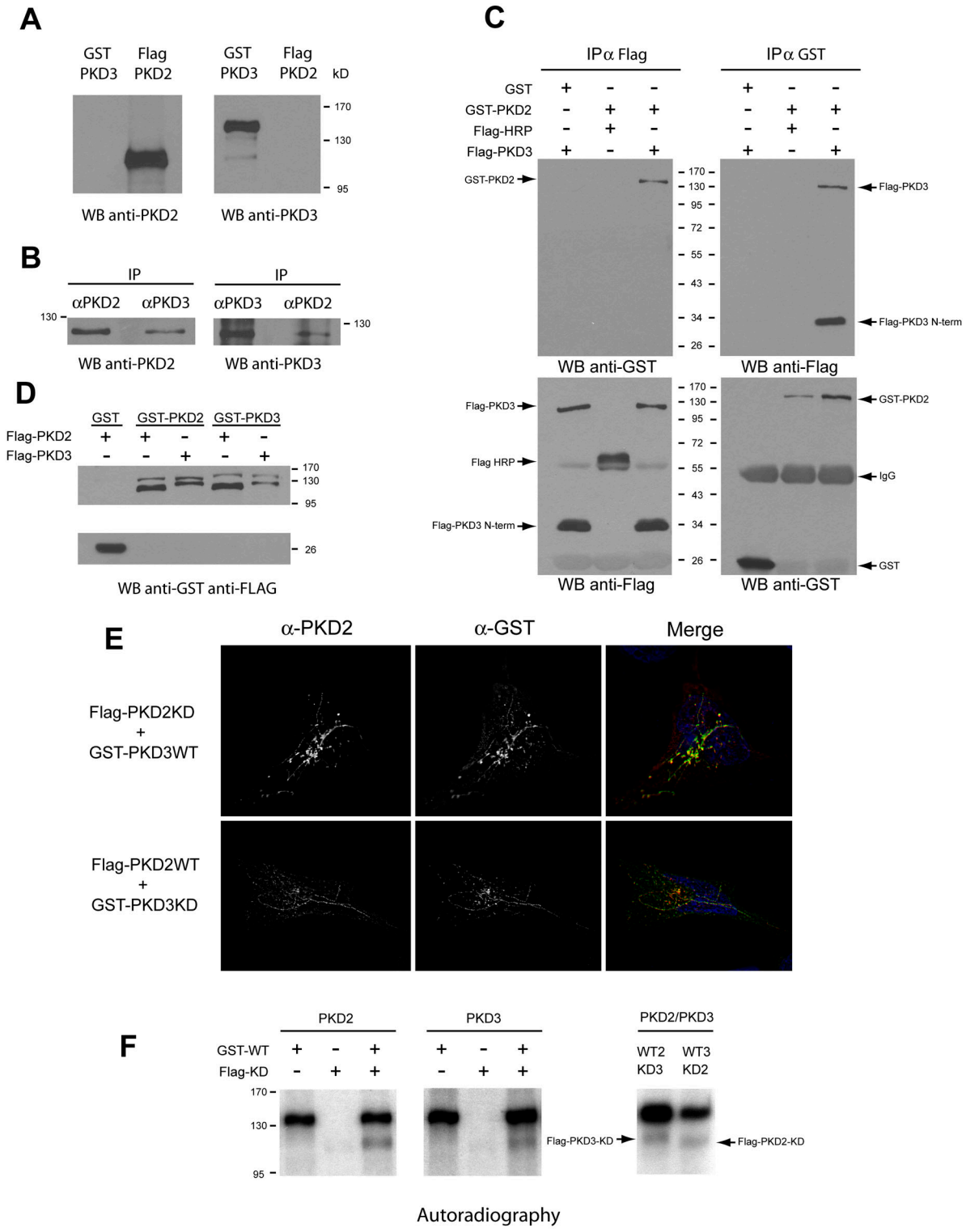

Figure 3. **PKD2 and PKD3 dimerize and transphosphorylate.** (A) Specificity of PKD2 and PKD3 antibodies. Pure recombinant Flag-PKD2 and GST-PKD3 were Western blotted with anti-PKD2 and -PKD3 antibodies. Anti-PKD2 antibody recognizes PKD2 (lane 2) and anti-PKD3 antibody recognize PKD3 (lane 3). (B) PKD2 and PKD3 interact. PKD2 or PKD3 was immunoprecipitated from HeLa cell lysates with specific antibodies and the precipitates blotted with anti-PKD2 antibody (lanes 1 and 2) or PKD3 antibody (lanes 3 and 4). (C) Exogenously expressed PKD2 and PKD3 interact. GST (lane 1) or GST-PKD2 (lanes 2 and 3) was coexpressed with Flag-HRP (lane 2) or FLAG-PKD3 (lanes 1 and 3) in HeLa cells. The cells were immunoprecipitated with anti-Flag antibody (top left) or anti-GST antibody (top right) and Western blotted with anti-GST or anti-Flag antibody, respectively. To verify that each tagged protein was expressed and immunoprecipitated, the Flag and the GST precipitates were respectively blotted with anti-Flag (bottom left) and anti-GST (bottom right). (D) PKD2 and PKD3 interact directly. Pure recombinant GST-tagged proteins were incubated in vitro with pure recombinant Flag-tagged proteins. After GST pull-down, the precipitates were Western blotted with anti-Flag antibody, followed by anti-GST antibody. (E) PKD2 and PKD3 colocalize on PKD-KD tubes. HeLa cells were cotransfected with Flag-PKD2-KD and GST-PKD3-WT (top) or with Flag-PKD2-WT and GST-PKD3-KD (bottom). The cells were visualized by fluorescence microscopy with anti-PKD2 and anti-GST antibody. (F) PKD2 and PKD3 transphosphorylate. Pure recombinant GST-PKD2-WT was incubated

and PKD3 dimerize in the cytoplasm before DAG-dependent recruitment to the TGN.

PKD1 in addition to autophosphorylation transphosphorylates other PKD1 molecules (Sanchez-Ruiloba et al., 2006). We therefore tested whether PKD2 and PKD3 share this property. Flag-PKD2-KD, Flag-PKD3-KD, GST-PKD2-WT, and GST-PKD3-WT were expressed in 293T cells and immunoprecipitated by specific antibodies. The isolated (soluble) Flag-tagged PKD-KD (2 or 3) was incubated with or without the GST-tagged kinases WT (2 or 3) attached to the beads in a kinase buffer. The phosphorylation status of the kinase-dead proteins by wild-type kinases was determined by SDS-PAGE followed by autoradiography. Our results reveal that PKD2 transphosphorylates other PKD2 molecules and also PKD3, and similarly PKD3 transphosphorylates PKD2 and other PKD3 molecules (Fig. 3 F).

A constitutively activated PKD converts TGN into small vesicles

If PKD depletion inhibits membrane fission then its overactivation should cause extensive vesiculation. A constitutively activated PKD containing a CAAX domain was generated to test this hypothesis. Proteins containing CAAX domain at their C-terminal can be prenylated, which confers a greater hydrophobicity and membrane anchoring (Choy et al., 1999; Wright and Philips, 2006). We reasoned that PKD-CAAX upon recruitment to the TGN through its C1domain (Maeda et al., 2001) will be inserted into the membrane via prenylation. This will retain activated PKD on TGN and hyperactivate the fission process. A constitutively activated PKD (PKD-CA) was generated by replacing Ser744 and Ser 748 with glutamic acid to mimic the phosphorylated form, as described by Iglesias et al. (1998). The kinase-dead form of PKD (PKD-KD) refers to PKD-K618N as described previously (Liljedahl et al., 2001).

HeLa cells stably expressing a GFP-tagged form of mannosidase II (MannII-GFP) (Sutterlin et al., 2005) were transfected with PKD-WT, PKD-CAAX-WT, PKD-CAAX-CA, or PKD-CAAX-KD. 24 h after transfection the cells were visualized with anti-GST antibodies to detect transfected cells, and the organization of Golgi apparatus was visualized with MannII-GFP (early Golgi) or an antibody against TGN46 (late Golgi). In cells transfected with PKD-CAAX-CA, the Golgi (cis Golgi as well as TGN) was found fragmented, whereas in cells transfected with PKD-WT or PKD-CAAX-KD the Golgi was unaffected (Fig. 4 A). In cells transfected with PKD-CAAX-WT, the Golgi was fragmented when expressed at high levels (Fig. 4 A, line 2). The recruitment of PKD to TGN requires DAG, which is inhibited by treatment of cells with fumonisin B1 (FB1) that lowers the intracellular pool of DAG (Baron and Malhotra, 2002). We found that depletion of DAG by FB1 inhibited the recruitment of PKD-KD and PKD-CAAX-KD to the Golgi membranes, and PKD-CAAX-CA mediated fragmentation of Golgi membranes (Fig. 4 B). Thus, the CAAX motif does not provide any specificity to PKD recruitment but simply anchors it to the TGN in a DAG-dependent manner.

To further ascertain the effects of constitutively activated PKD on the organization of Golgi membranes, the following constructs were coexpressed in HeLa cells; sialyltransferase (ST)-HRP and either PKD-WT, PKD-CAAX-WT, PKD-CAAX-CA, or PKD-CAAX-KD. The cells were fixed and thin sections visualized by immunoelectron microscopy with anti-HRP antibody to visualize the resident enzyme ST of TGN (Fig. 5, A–D, left panel), or anti-TGN46 antibody, which is a cargo protein of the TGN-to-cell surface pathway (Fig. 5, E–H, right panel). There was a definitive increase in the number of vesicles in the vicinity of Golgi stacks in cells expressing either PKD-CAAX-WT or PKD-CAAX-CA compared with PKD-CAAX-KD or PKD-WT (Fig. 5). A quantitation of these images revealed a five- to seven-fold increase in the number of vesicles containing TGN46 in cells expressing CAAX variants of PKD-WT or the constitutively activated form compared with PKD-WT or PKD-CAAX-KD (Table I). Interestingly, there was a 20- and 25-fold increase in the number of ST-containing vesicles in cells expressing PKD-CAAX-WT and PKD-CAAX-CA, respectively, compared with PKD-WT or PKD-CAAX-KD. Thus, overexpression of the wild-type or constitutively activated form of PKD hyperactivates the fission reaction, and causes extensive vesiculation of the TGN. We suggest that this reaction first generates the normal cargo (TGN46 containing) transport vesicles, but the reaction continues and consumes domains containing Golgi resident enzymes that are ordinarily excluded from participating in TGN-to-cell surface transport reaction.

Conclusion

Our findings clearly demonstrate the regulation of membrane fission by PKD. But how does PKD regulate membrane fission? As mentioned above, PKD is recruited by a DAG-dependent manner to the TGN and then activated by PKCη. We suggest that a PKD-dependent increase in local concentration of DAG separates transport carriers from the TGN by periplasmic fusion. This coat- and dynamin-independent (fission) reaction is therefore fundamentally different from the process of COPI, COPII, and clathrin-coated vesicle biogenesis.

Materials and methods

RT-PCR

Total RNA was extracted from HeLa cells with Nucleospin RNAII (Machery-Nagel) and reverse-transcribed with Titanium One-Step RT-PCR kit (Clontech Laboratories, Inc.) according to the manufacturer's instructions.

Quantitative RT-PCR

Reverse transcription was performed using 1 μg of purified RNA, oligo dT, and SuperScript III reverse transcriptase (Invitrogen) in a 20-μl reaction.

Amplification of each specific transcript was performed using RT^2 PCR primer Set (SuperArray). Plasmids containing cDNAs for each specific PKD isoform were used as standards for real-time quantitative PCR amplification (Q-PCR). These plasmids were 10-fold serially diluted and used as

alone (lane 1) or mixed with either Flag-PKD2-KD (lane 3) or Flag-PKD3-KD (lane 7) for in vitro kinase assays. Similarly, GST-PKD3-WT was incubated alone (lane 4) or mixed with Flag-PKD3-KD (lane 6) or Flag-PKD2-KD (lane 8). The lack of kinase activity of Flag-PKD2-KD and Flag-PKD3-KD is shown in lanes 2 and 5, respectively.

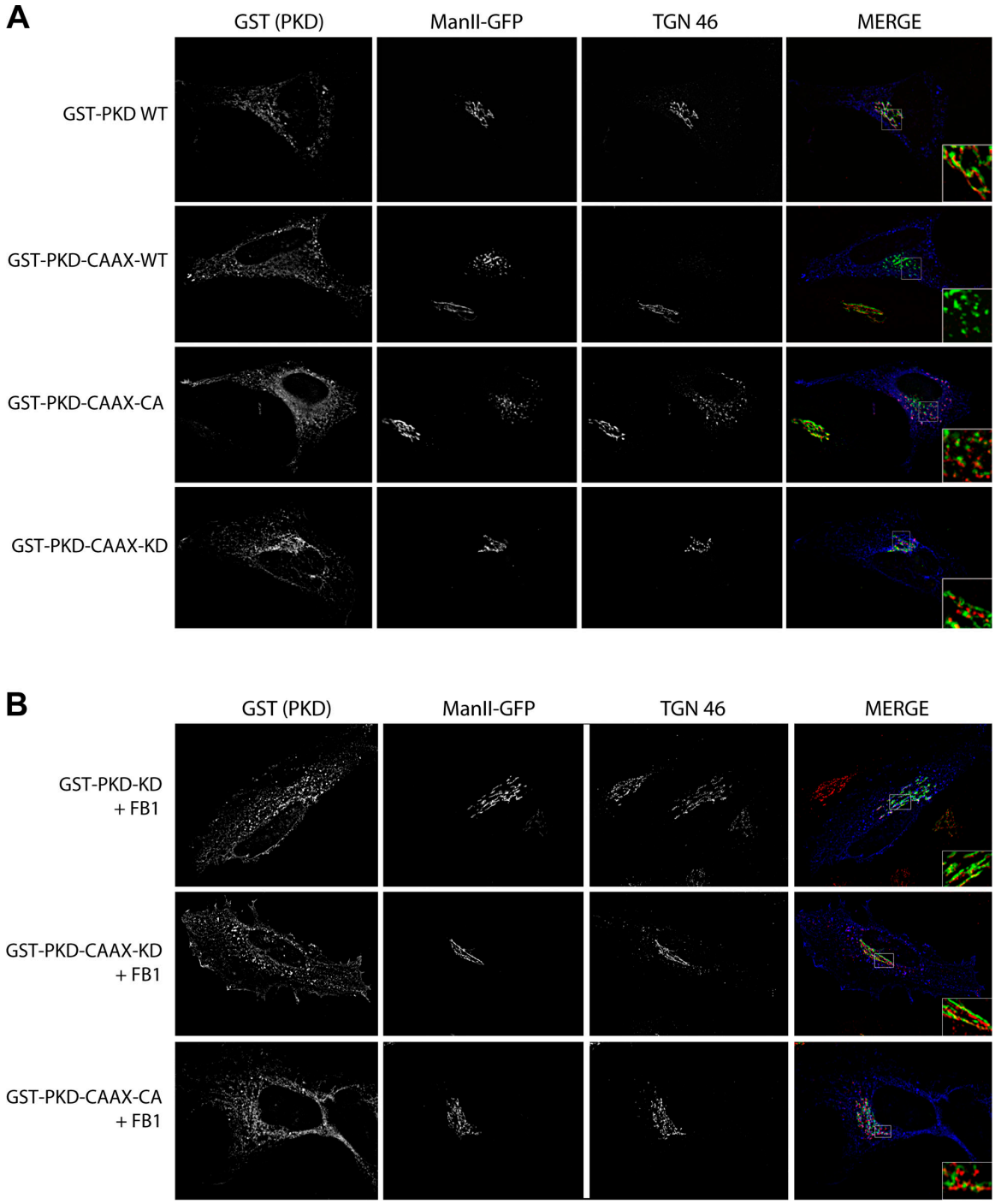

Figure 4. **Expression of an overactivated form of PKD fragments the Golgi apparatus.** (A) HeLa cells stably expressing MannII-GFP were transfected with GST-tagged PKD WT, PKD-CAAX-WT, PKD-CAAX-CA, or PKD-CAAX-KD. The localization of PKD and the organization of Golgi membranes were monitored by fluorescence microscopy with anti-GST and TGN46 antibody, respectively. (B) PKD-CAAX-CA–dependent Golgi fragmentation requires DAG. HeLa MannII-GFP cells were pretreated with fumonisin1 (FB1) 24 h before transfection with PKD constructs. 24 h after transfection, cells were fixed and stained with anti-GST and anti-TGN46 antibodies.

templates for the Q-PCR to generate standard curves (ranging from 10^2 to 10^5 copies/μl). Real-time Q-PCR assays were performed with an Mx4000 Multiplex Quantitative QPCR System (Stratagene). Reactions were performed using 200-nM primers, 1 μl template/25 μl PCR reaction and the iTaq SYBR Green Supermix with ROX (Bio-Rad). A two-step PCR method (denaturation at 95°C for 30 s and annealing/extension at 60°C for 1 min) was used. Each assay included the analysis of the samples in duplicates. In addition, samples were run at least three times to check for interassay variability. Melting curve analyses were performed on all PCR reactions to check for specificity of the amplification. Real-time qRT-PCR analyses for β-actin were included as housekeeping genes to normalize the data.

Antibodies

Antibodies in this study included goat anti-GST (GE Healthcare), rabbit anti-GST (AbCam), sheep anti–human TGN46 (AbD Serotec), rabbit affinity-purified anti-PKD3 (Bethyl), rabbit affinity-purified anti-PKD2 (Bethyl) monoclonal anti-β-actin (Sigma-Aldrich), monoclonal anti-Flag (Sigma-Aldrich), AMCA donkey anti–rabbit (Jackson ImmunoResearch Laboratories), and Texas

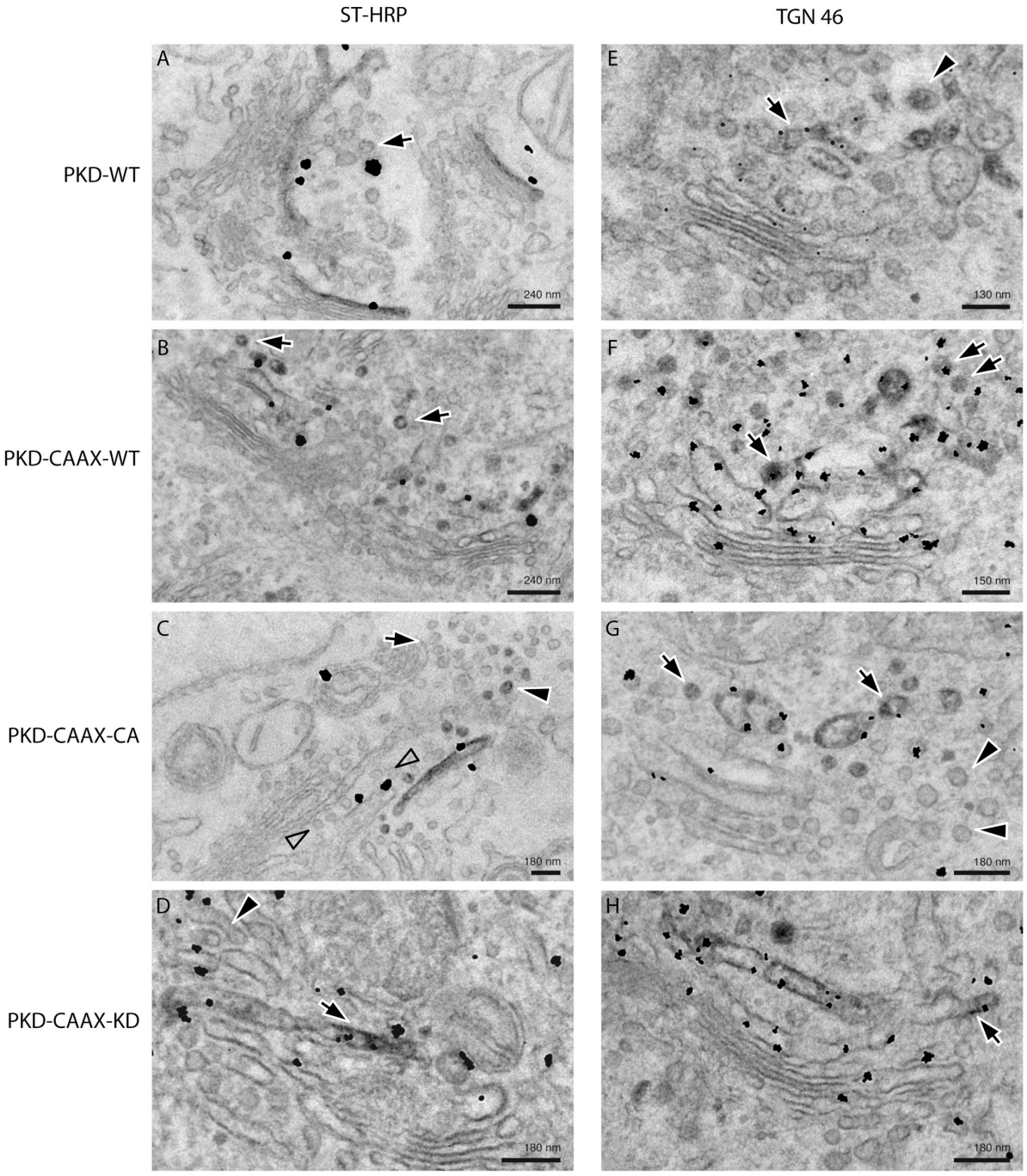

Figure 5. **Analysis of HeLa cells transfected with PKD CAAX isoforms by electron microscopy.** HeLa cells transfected with PKD-WT, PKD-CAAX-WT, PKD-CAAX-CA, or PKD-CAAX-KD alone (right) or with ST-HRP (left) were processed for electron microscopy. (A) Gold particles indicating the presence of PKD-WT reveal its presence at the TGN (where ST-HRP is also visible). Few vesicles lacking ST-HRP were also visible in sections (arrow). (B) Expression of PKD-CAAX-WT increased the number of ST-HRP–positive vesicles (arrows). (C) PKD-CAAX-CA induced an increase in the number of vesicles with ST-HRP (arrowheads); however, number of unlabeled vesicles also increases (arrows). Row of vesicles (empty arrows) between ST-positive cisterna and the rest of the stack may represent cisterna consumed by vesicles, and this also might explain why ST-positive cisterna appears to be peeling off. (D) Cells expressing PKD-CAAX-KD exhibit regular trans-Golgi cisterna (arrow) labeled with ST-HRP. Some tubular structures (presumably TGN) are also visible at the trans-face of the Golgi (arrowhead). (E) Cells expressing PKD-WT exhibit regular TGN with both tubular (arrow) and vesicles (arrowhead). PKD is detected at the TGN46-positive membranes. (F) PKD-CAAX-WT induced an increase in the number of TGN46-positive vesicles (arrows). (G) Expression of PKD-CAAX-CA induced extensive vesiculation of the Golgi apparatus. Both TGN46-positive (arrows) and TGN46-negative (arrowheads) vesicles increased in numbers under these conditions. PKD is detected at the TGN46-positive membranes. (H) Long TGN46-positive (arrows) tubular structures were detected in PKD-CAAX-KD–expressing cells without any obvious increase in number of vesicles.

red donkey anti–sheep (Jackson ImmunoResearch Laboratories). The monoclonal antibody 8G5F11, which recognizes the extracellular domain of VSV-G, was provided by Dr. Douglas Lyles (Wake Forest University School of Medicine, Winston-Salem, NC).

Cell culture and transfection

293-T cells, HeLa cells, and the cell line stably expressing a GFP-tagged form of mannosidase II (HeLa MannII-GFP) were grown in complete medium consisting of DME (Cellgro) containing 10% FCS and supplemented

Table I. **Quantitation of the ST-HRP– and TGN-positive vesicles**

	PKD-WT	PKD-CAAX-WT	PKD-CAAX-CA	PKD-CAAX-KD
ST-HRP vesicles	0.30 ± 0.48	5.90 ± 1.07	7.40 ± 2.57	0.45 ± 0.25
TGN46 vesicles	1.50 ± 0.50	7.22 ± 2.40	6.85 ± 2.80	1.20 ± 0.90

Bars represent mean ± SD of the number of vesicles and show that they originate from the TGN in cells expressing PKD-CAAX-CA and PKD-CAAX-WT.

with 0.8 mg/ml of geneticin for HeLa MannII-GFP at 37°C in a 7% CO_2 incubator. The cells were transfected with FuGene 6 (Roche) or Lipofectamine 2000 (Invitrogen) following the manufacturer's recommendations.

siRNA transfection
The day before transfection, HeLa cells were plated in order to ensure 50% confluency on the day of transfection. Knockdown transfections were performed using 80 nM of purified siRNA and Lipofectamine 2000 according to the manufacturer's protocol. For the VSV-G transport assay, specific targeting siRNA and siGlo Risc free-labeled nonspecific siRNA were mixed (ratio 4:1) with a final concentration of 100 nM. siRNAs controls were from Dharmacon. The siRNA PKD3 and the siRNA PKD2 are Silencer-validated siRNAs from Ambion.

ssHRP and PLAP secretion assay
30 h after transfection with siRNA, the cells were cotransfected with the SS-HRP-Flag and the pSEAP2-basic (Clontech Laboratories, Inc.) plasmid (carrying PLAP cDNA), using Lipofectamine 2000 (Invitrogen). 30 μl of extracellular media was harvested 48 h after the initial siRNA transfection. HRP activity was measured using enhanced chemiluminescence (ECL) as described previously (Bard et al., 2006). PLAP activity in the medium and in the cells was measured using the Phospha-Light System (Applied Biosystems) following the manufacturer's protocol. PLAP activity inside the cells was normalized by total protein concentration and used to normalize both HRP and PLAP secreted into the medium.

VSV-G transport assay
30 h after transfection with siRNA, the cells were transfected with *ts*045VSV-G-GFP construct and cultured at 40°C for 20 h. 100 μg/ml of cycloheximide was then added before a 2-h incubation at 20°C. After an incubation at 32°C for 40 min the cells were harvested with a cell dissociation buffer (Invitrogen) and fixed with 4% paraformaldehyde. After blocking with PBS containing 1.5% serum and 0.1% sodium azide, the labeling of surface VSV-G–GFP was performed for a 30-min incubation at 4°C with the anti-VSV-G mAb 8G5F11, which is specific for the extracellular domain of VSV-G. After washings with the blocking buffer, the cells were incubated with the secondary (APC)-labeled anti–mouse IgG antibody (Jackson ImmunoResearch Laboratories) for 30 min at 4°C. After washing, the cells were analyzed on a FACScalibur flow cytometer (BD Biosciences). The amount of VSV-G present at the cell surface (APC positive) of cells transfected with both siRNA (cy3 positive) and VSV-G (GFP positive) after subtracting the background was normalized by the GFP intensity.

Immunoprecipitation
Transfected 293-T cells or HeLa cells were lysed in 50 mM Tris, pH 7.4, 150 mM NaCl, 1% Triton X-100, and protease inhibitors for 30 min at 4°C. After centrifugation at 13,000 rpm for 10 min, protein concentrations were measured in the lysates. 100 μg of extracts were incubated with the primary antibody (1:100) at 4°C and after 2 h, 30 μl of G-Sepharose beads (GE Healthcare) were added for 1 h. Immobilized proteins were released by boiling in Laemmli buffer and analyzed by SDS-PAGE. For Flag-tagged proteins, 100 μg of cell lysates were incubated with anti-Flag M2 affinity gel and eluted with 3×Flag peptide following the manufacturer's instructions (Sigma-Aldrich).

In vitro kinase assay
An equal amount of the indicated proteins purified by immunoprecipitation from transfected 293-T cells was incubated for 10 min at 32°C in a buffer containing 50 mM Tris-HCl, 30 mM $MgCl_2$, 0,3 mM ATP, 2 mM DTT, 0.2 μM PdBu, and 5 μCi ATPγP^{32}. The reaction was stopped by addition of 6× SDS sample buffer and the samples were processed for SDS-PAGE and autoradiography.

In vitro binding assay
After immunoprecipitation with anti-GST antibody from transfected 293-T cell lysates, the purified GST-tagged proteins bound to the beads were incubated with equal amount of purified Flag-tagged proteins for 2 h at 4°C in 300 μl of PBS containing 0.1% Triton X-100 and 0.2%BSA. After extensive washes in the same buffer, the precipitates were eluted in 1× SDS sample buffer and processed for Western blotting.

PKD-CAAX constructs cloning
PKD-CAAX-CA, PKD-CAAX-WT, and PKD-CAAX-KD were cloned by PCR using GST-PKD-CA, GST-PKD-WT, and GST-PKD-KD, respectively, as templates as previously described (Maeda et al., 2001). The CAAX motif was appended by using a reverse primer containing the nucleotides coding for the CAAX motif MVLC: 5′-AAATCTAGAAAGCTTTCACATAACGAGACAGAGGATG-CTGACACGCTCACTG-3′.

Immunofluorescence
24 h after transfection, HeLa cells expressing MannII-GFP grown on coverslips were fixed with 4% formaldehyde in PBS for 10 min, blocked, and permeabilized with blocking buffer (0.05% Saponin and 0.2% BSA in PBS) for 20 min. The coverslips were incubated with primary antibodies diluted in blocking buffer for 2 h, washed, incubated with secondary antibodies diluted in blocking buffer for 1 h, washed, mounted using Fluor Save Reagent (Calbiochem), and visualized with a Nikon Eclipse TE2000-U microscope. Pictures were taken using MetaMorph software and deconvolved using AutoVisualize+AutoDeblur 9.3 software. The pictures were then opened in ImageJ v1.37 and Adobe Photoshop.

Electron microscopy
HeLa cells were depleted of both PKD2 and PKD3 as described above. The cells were transfected with SS-HRP and processed for immunoelectron microscopy, and HRP was visualized by staining with DAB and H_2O_2 as described previously (Polishchuk et al., 2000). HeLa cells were transfected with GST-tagged PKD WT, PKD-CAAX-CA, PKD-CAAX-WT, or PKD-CAAX-KD. Cells were fixed in the mixture of 4% paraformaldehyde and 0.5% glutaraldehyde, washed, and labeled with anti-TGN46–specific antibody followed by an antibody conjugated with peroxidase as described previously (Polishchuk et al., 2000). Then cells were incubated with polyclonal antibody against GST and subsequently with Nanogold-conjugated Fab fragment of anti–rabbit IgG. Nanogold particles were enhanced using the manufacturer's kit (Nanoprobes). ST-HRP-expressing cells were incubated directly with DAB and H_2O_2 (Polishchuk et al., 2000) and then labeled with anti-GST antibody as described above. Cells were then embedded in Epon 812 and thin sections visualized in a Tecnai-12 electron microscope (FEI, Philips). Images were taken using an Ultra View CCD digital camera. Morphometric analysis of Golgi stacks was performed in 20 cells for each experimental condition using the ANALYSIS software.

Tubular profiles were defined as HRP-positive structures with length twice or more higher than thickness.

Statistics
The statistical significance of the difference between means was determined using the *t* test. Differences were considered significant at $P < 0.01$.

This work was supported by National Institutes of Health grants (GM46224 and GM53747), and a senior investigator award from the Sandler's program for Asthma research to V. Malhotra. C. Bossard was supported by a Human Frontier Science Program postdoctoral fellowship. R.S. Polishchuk was supported by Telethon EM Facility Grant GTF05007 and Telethon Rersearch Grant GGP05044.

Submitted: 27 March 2007
Accepted: 15 November 2007

References

Audhya, A., M. Foti, and S.D. Emr. 2000. Distinct roles for the yeast phosphatidylinositol 4-kinases, Stt4p and Pik1p, in secretion, cell growth, and organelle membrane dynamics. *Mol. Biol. Cell.* 11:2673–2689.

Bard, F., and V. Malhotra. 2006. The formation of TGN-to-plasma-membrane transport carriers. *Annu. Rev. Cell Dev. Biol.* 22:439–455.

Bard, F., L. Casano, A. Mallabiabarrena, E. Wallace, K. Saito, H. Kitayama, G. Guizzunti, Y. Hu, F. Wendler, R. Dasgupta, et al. 2006. Functional genomics reveals genes involved in protein secretion and Golgi organization. *Nature.* 439:604–607.

Baron, C.L., and V. Malhotra. 2002. Role of diacylglycerol in PKD recruitment to the TGN and protein transport to the plasma membrane. *Science.* 295:325–328.

Choy, E., V.K. Chiu, J. Silletti, M. Feoktistov, T. Morimoto, D. Michaelson, I.E. Ivanov, and M.R. Philips. 1999. Endomembrane trafficking of ras: the CAAX motif targets proteins to the ER and Golgi. *Cell.* 98:69–80.

Diaz Anel, A.M., and V. Malhotra. 2005. PKCeta is required for beta1gamma2/beta3gamma2- and PKD-mediated transport to the cell surface and the organization of the Golgi apparatus. *J. Cell Biol.* 169:83–91.

Fugmann, T., A. Hausser, P. Schoffler, S. Schmid, K. Pfizenmaier, and M.A. Olayioye. 2007. Regulation of secretory transport by protein kinase D-mediated phosphorylation of the ceramide transfer protein. *J. Cell Biol.* 178:15–22.

Godi, A., A. Di Campli, A. Konstantakopoulos, G. Di Tullio, D.R. Alessi, G.S. Kular, T. Daniele, P. Marra, J.M. Lucocq, and M.A. De Matteis. 2004. FAPPs control Golgi-to-cell-surface membrane traffic by binding to ARF and PtdIns(4)P. *Nat. Cell Biol.* 6:393–404.

Hausser, A., P. Storz, S. Martens, G. Link, A. Toker, and K. Pfizenmaier. 2005. Protein kinase D regulates vesicular transport by phosphorylating and activating phosphatidylinositol-4 kinase IIIbeta at the Golgi complex. *Nat. Cell Biol.* 7:880–886.

Hausser, A., G. Link, M. Hoene, C. Russo, O. Selchow, and K. Pfizenmaier. 2006. Phospho-specific binding of 14-3-3 proteins to phosphatidylinositol 4-kinase III beta protects from dephosphorylation and stabilizes lipid kinase activity. *J. Cell Sci.* 119:3613–3621.

Iglesias, T., R.T. Waldron, and E. Rozengurt. 1998. Identification of in vivo phosphorylation sites required for protein kinase D activation. *J. Biol. Chem.* 273:27662–27667.

Jamora, C., P.A. Takizawa, R.F. Zaarour, C. Denesvre, D.J. Faulkner, and V. Malhotra. 1997. Regulation of Golgi structure through heterotrimeric G proteins. *Cell.* 91:617–626.

Jamora, C., N. Yamanouye, J. Van Lint, J. Laudenslager, J.R. Vandenheede, D.J. Faulkner, and V. Malhotra. 1999. Gbetagamma-mediated regulation of Golgi organization is through the direct activation of protein kinase D. *Cell.* 98:59–68.

Liljedahl, M., Y. Maeda, A. Colanzi, I. Ayala, J. Van Lint, and V. Malhotra. 2001. Protein kinase D regulates the fission of cell surface destined transport carriers from the trans-Golgi network. *Cell.* 104:409–420.

Lipardi, C., L. Nitsch, and C. Zurzolo. 2000. Detergent-insoluble GPI-anchored proteins are apically sorted in fischer rat thyroid cells, but interference with cholesterol or sphingolipids differentially affects detergent insolubility and apical sorting. *Mol. Biol. Cell.* 11:531–542.

Lisanti, M.P., A. Le Bivic, A.R. Saltiel, and E. Rodriguez-Boulan. 1990. Preferred apical distribution of glycosyl-phosphatidylinositol (GPI) anchored proteins: a highly conserved feature of the polarized epithelial cell phenotype. *J. Membr. Biol.* 113:155–167.

Maeda, Y., G.V. Beznoussenko, J. Van Lint, A.A. Mironov, and V. Malhotra. 2001. Recruitment of protein kinase D to the trans-Golgi network via the first cysteine-rich domain. *EMBO J.* 20:5982–5990.

Polishchuk, R.S., E.V. Polishchuk, P. Marra, S. Alberti, R. Buccione, A. Luini, and A.A. Mironov. 2000. Correlative light-electron microscopy reveals the tubular-saccular ultrastructure of carriers operating between Golgi apparatus and plasma membrane. *J. Cell Biol.* 148:45–58.

Rykx, A., L. De Kimpe, S. Mikhalap, T. Vantus, T. Seufferlein, J.R. Vandenheede, and J. Van Lint. 2003. Protein kinase D: a family affair. *FEBS Lett.* 546:81–86.

Sanchez-Ruiloba, L., N. Cabrera-Poch, M. Rodriguez-Martinez, C. Lopez-Menendez, R.M. Jean-Mairet, A.M. Higuero, and T. Iglesias. 2006. Protein kinase D intracellular localization and activity control kinase D-interacting substrate of 220-kDa traffic through a postsynaptic density-95/discs large/zonula occludens-1-binding motif. *J. Biol. Chem.* 281:18888–18900.

Sutterlin, C., R. Polishchuk, M. Pecot, and V. Malhotra. 2005. The Golgi-associated protein GRASP65 regulates spindle dynamics and is essential for cell division. *Mol. Biol. Cell.* 16:3211–3222.

Takizawa, P.A., J.K. Yucel, B. Veit, D.J. Faulkner, T. Deerinck, G. Soto, M. Ellisman, and V. Malhotra. 1993. Complete vesiculation of Golgi membranes and inhibition of protein transport by a novel sea sponge metabolite, ilimaquinone. *Cell.* 73:1079–1090.

Walch-Solimena, C., and P. Novick. 1999. The yeast phosphatidylinositol-4-OH kinase pik1 regulates secretion at the Golgi. *Nat. Cell Biol.* 1:523–525.

Wright, L.P., and M.R. Philips. 2006. Thematic review series: lipid posttranslational modifications. CAAX modification and membrane targeting of Ras. *J. Lipid Res*. 47:883–891.

Yeaman, C., M.I. Ayala, J.R. Wright, F. Bard, C. Bossard, A. Ang, Y. Maeda, T. Seufferlein, I. Mellman, W.J. Nelson, and V. Malhotra. 2004. Protein kinase D regulates basolateral membrane protein exit from trans-Golgi network. *Nat. Cell Biol.* 6:106–112.